Evidence of a Spin Resonance Mode in the Iron-Based Superconductor $Ba_{0.6}K_{0.4}Fe_2As_2$ from Scanning Tunneling Spectroscopy

Lei Shan,[1,*] Jing Gong,[1] Yong-Lei Wang,[1] Bing Shen,[1] Xingyuan Hou,[1] Cong Ren,[1] Chunhong Li,[1] Huan Yang,[1,2]
Hai-Hu Wen,[1,2] Shiliang Li,[1] and Pengcheng Dai[1,3]

[1]*National Laboratory for Superconductivity, Beijing National Laboratory for Condensed Matter Physics, Institute of Physics,
Chinese Academy of Sciences, Beijing 100190, China*
[2]*National Laboratory of Solid State Microstructures and Department of Physics, Nanjing University, Nanjing 210093, China*
[3]*Department of Physics and Astronomy, The University of Tennessee, Knoxville, Tennessee 37996-1200, USA*
(Received 3 November 2011; published 31 May 2012)

We used high-resolution scanning tunneling spectroscopy to study the hole-doped iron pnictide superconductor $Ba_{0.6}K_{0.4}Fe_2As_2$ ($T_c = 38$ K). Features of a bosonic excitation (mode) are observed in the measured quasiparticle density of states. The bosonic features are intimately associated with the superconducting order parameter and have a mode energy of ~ 14 meV, similar to the spin resonance measured by inelastic neutron scattering. These results indicate a strong electron-spin excitation coupling in iron pnictide superconductors, similar to that in high-T_c copper oxide superconductors.

In conventional superconductors, the electron-phonon interaction responsible for electron pairing and superconductivity was unequivocally established by tunneling and neutron scattering experiments, where dips in the second derivative of the tunneling current d^2I/dV^2 correspond to phonon modes observed by inelastic neutron scattering experiments [1–3]. To obtain the equivalent information for high-transition temperature (high-T_c) superconductors, it is important to identify the electron-boson coupling [4] and its connections to superconductivity. For bosonic "pairing glue" mediated superconductors, the "glue" may arise from the usual electron-phonon interactions [5] or the exchange of particle-hole spin fluctuations characterized by the imaginary part of the dynamic susceptibility, $\chi''(Q, \omega)$, which is seen in inelastic magnetic neutron scattering measurements [6–9]. For electron-doped high-T_c copper oxide superconductors, tunneling experiments using scanning tunneling microscopy on $Pr_{0.88}LaCe_{0.12}CuO_4$ have identified a bosonic excitation at an energy (10.5 meV) consistent with the neutron spin resonance [10–12], thus providing evidence that spin fluctuations mediate superconductivity [13]. The spin resonance mode has also been observed in tunneling experiments of hole-doped copper oxide superconductors [14–16], and quantitative analysis suggested that quasiparticle interactions with this mode are important for superconductivity. In the case of iron-based superconductors [17–22], spin fluctuations have been suggested to be responsible for superconductivity through sign reversed quasiparticle excitations between the isotropic hole pockets near Γ and electron pockets near M [23] (the so-called $s_{\pm}$-wave). Although the discovery of a neutron spin resonance in optimally hole-doped $BaFe_2As_2$ [24,25] and a bosonic structure in scanning tunneling spectroscopy (STS) of $SmFeAsO_{1-x}F_x$ [26] are consistent with spin fluctuation

mediated $s_{\pm}$-wave superconductivity, these measurements were carried out on different classes of materials. Therefore, there is no direct experimental evidence connecting neutron spin resonance to the bosonic features in STS of the same material.

In this Letter, we report high-resolution STS studies of the optimally hole-doped iron-based high-T_c superconductor $Ba_{0.6}K_{0.4}Fe_2As_2$ ($T_c = 38$ K). We found that the second derivative of the tunneling current d^2I/dV^2 shows clear high-bias (eV $> \Delta$) features at energies of ~ 14 meV, in good agreement with the neutron spin resonance mode [24,25]. The ratio of the mode energy and superconducting gap suggests that the resonance mode is a magnetic exciton as observed in copper oxide superconductors, indicating that spin fluctuations are important for high-T_c superconductivity.

The nearly optimally doped $Ba_{0.6}K_{0.4}Fe_2As_2$ ($T_c = 38$ K) single crystals studied here were grown with the self-flux method [27]. The spatially resolved tunneling experiments were carried out on a low-temperature scanning tunneling microscope that was constructed in house [28,29]. A single crystalline sample was cold-cleaved *in situ* and then immediately inserted into the microscope, which had been maintained at the desired temperature.

Figure 1(a) shows typical tunneling spectra (dI/dV vs. V) at temperatures below and above T_c. At $T = 3.5$ K, there were two sharp coherence peaks accompanied by zero conductance around zero bias voltage, indicating a superconducting gap. Upon warming up to $T = 40$ K, the coherence peaks disappeared and the spectrum became featureless. More features can be seen in the spectrum shown in Fig. 1(b), which is an average over a 16.7 nm × 8.4 nm region measured at 2.1 K. As indicated by the gray vertical lines, in addition to a larger gap of 8.4 meV, a smaller gap of 3.5 meV appears as kinks on the spectrum.
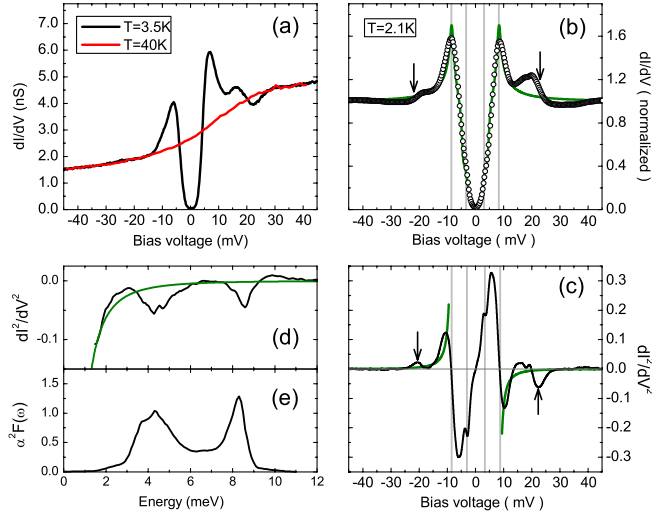
FIG. 1 (color online).   (a) Typical tunneling spectra measured below (black) and above (red) T_c. (b) Normalized spectrum averaged over an area of $16.7 \text{ nm} \times 8.4 \text{ nm}$. The features of two superconducting gaps are indicated by gray vertical lines. Black arrows indicate the hump-dip structures mentioned in the text, and the green line is a fit to two-gap weak-coupling BCS theory. Spectra were taken with a fixed junction resistance of $0.25 \text{ G}\Omega$. (c) Second derivative of the tunneling current calculated from the data presented in (b). The green line is a BCS calculation. (d) The black curve is the relationship between d^2I/dV^2 vs. $(eV - \Delta)$ obtained on a conventional strong-coupling superconductor Pb in an energy window outside the superconducting gap Δ [3]. The green line is a BCS curve. (e) Electron-phonon spectral function of Pb [3].

The two superconducting gaps are also distinguished in the second derivative of the tunneling current as shown in Fig. 1(c). This two-gap structure can be fitted very well to the BCS theory by combining the spectral contributions from the two superconducting gaps as shown in Fig. 1(b), in good agreement with our previous measurements [28,29]. In general, STS detects the integrated quasiparticle density of states (DOS) over all Fermi surfaces with a momentum-dependent spectral weight. For a real tunneling process, the spectral weight contribution from certain momentum directions may dominate depending on the tunneling matrix element and the possible scattering from the surface layer [30]. This is why, for iron-based superconductors, only one gap can be detected on some surfaces [26,31–34], whereas multiple gaps can be observed on other surfaces [28,29,35].

Beyond previous measurements [28,29], the most interesting finding here is a hump-dip structure located outside the coherence peaks, as indicated by black arrows in Fig. 1(b). In previous work [29], our studied energy window was limited to ± 20 meV to avoid possible disturbance of higher voltage to the tunnel junctions. In that case, only the initial part of the hump-dip structure could be seen (see Figs. 2,4 in Ref. [29]). For superconductors

with a clean superconducting DOS, one should observe such fine structures in the tunneling spectra [36]. As shown in Fig. 1(b), the hump-dip structure is beyond weak-coupling BCS theory, but it is similar to the DOS feature of conventional strong-coupling superconductors. Figure 1(d) shows the second derivative of the tunneling current (d^2I/dV^2 vs. V) of Pb, where only the positive-bias part is plotted for clarity. By comparing to the BCS curve (in green), one can see two dips ascribed to the peaks in the phonon density of states $F(\omega)$ (phonon modes) following Eliashberg strong-coupling theory [Fig. 1(e)] [37,38]. High-bias features in tunneling spectra were also observed in copper oxide superconductors [10,14], which were ascribed to a strong electronic coupling to spin resonance modes both by qualitative analyses [10,12,14] and quantitative Eliashberg calculations [15,16]. The d^2I/dV^2 vs. V curve obtained for $\text{Ba}_{0.6}\text{K}_{0.4}\text{Fe}_2\text{As}_2$ also shows a distinct dip at the bias voltage (and a peak at corresponding negative bias) well above the gap edge as shown in Fig. 1(c). From Figs. 1(a)–1(c), we see that this high-bias feature is weaker at negative bias than that at positive bias. Analogous to that of Pb and copper oxides superconductors, the dip shown in Fig. 1(c) in $\text{Ba}_{0.6}\text{K}_{0.4}\text{Fe}_2\text{As}_2$ may be related to some bosonic modes.

Figure 2(a) shows a series of tunneling spectra recorded along a line with an interval of 5.4 Å, indicating more homogeneous electronic states than those of copper oxide superconductors [39]. We present in Fig. 2(b) the statistics
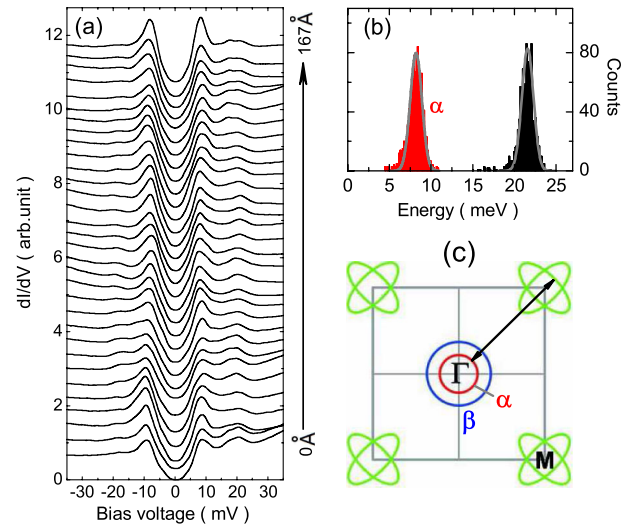

FIG. 2 (color online).   (a) Spatially-resolved tunneling spectra recorded along a line of 16.7 nm on the cleaved surface of a single crystal of $\text{Ba}_{0.6}\text{K}_{0.4}\text{Fe}_2\text{As}_2$. (b) A histogram of the occurrences of the larger gap Δ (red) and the dip E_{dip} (black), which were observed in the same region mentioned in Fig. 1. (c) Schematic diagram of the Fermi surface pockets of $\text{Ba}_{0.6}\text{K}_{0.4}\text{Fe}_2\text{As}_2$ (α-hole and β-hole pockets centered at Γ point and electron pocket around M point). The black arrow indicates the nesting vector between the α-hole pocket and the electron pocket.

of the larger superconducting gap (Δ) around 8.4 meV
mentioned above and the dip energy (E_{dip}) determined
from a high-resolution d^2I/dV^2 map of the 16.7 nm $\times$
8.4 nm region. In the superconducting state of a strong-
coupling superconductor, a bosonic mode will appear in
tunneling spectra at an energy offset by the gap; i.e.,
$\Omega = E_{\text{dip}} - \Delta$ in which Ω is the mode energy. In this
way, we found a mode energy of $\Omega \approx 14$ meV connecting
the larger gap around 8.4 meV mentioned above and the
dip indicated in Fig. 1(c). For all studied regions, Ω was
approximately 13–14 meV, which is very close to the
energy of the neutron spin resonance mode of $\omega \approx$
14 meV as measured by neutron scattering both in poly-
crystalline $Ba_{0.6}K_{0.4}Fe_2As_2$ [24] and in single crystalline
$Ba_{0.67}K_{0.33}Fe_2As_2$ [25]. On the other hand, compared with
angle resolved photoemission (ARPES) data [40,41], the
gap around 8.4 meV observed here stems mostly from the
inner hole pocket in momentum space as indicated by α in
Fig. 2(c). In fact, ARPES data show that the electron Fermi
surface centered at the M point also has a gap with a similar
magnitude to that of the α pocket. However, because the
tunneling rate along the z axis is suppressed with increas-
ing in-plane momentum [42], the STS measurements pre-
sented here are more sensitive to states near the Γ point. We
note that the neutron spin resonance was observed at the
nesting vector between the α pocket and the electron
pocket, and the mode energy derived from the tunneling
data is also related to the nested Fermi pockets. This gives
further evidence that the mode observed here may originate
from the neutron spin resonance mode, similar to the case
of copper oxide superconductors [10,12,14–16].

For a weak-coupling BCS superconductor, the pairing
strength ($\triangle$) is assumed to be a real constant. For a strong-
coupling superconductor, a complex and strongly energy-
dependent gap function [$\triangle(E)$] is induced by a realistic
electron-boson interaction, which is responsible for the fine
features of the bosonic excitations in the tunneling spectra.
To test the relationship between the bosonic features and
the superconducting order parameter from the STS data,
we studied the temperature and local impurity dependen-
cies of the tunneling spectra. As shown in Fig. 3(a), the
bosonic-excitation feature in the spectra became weak with
increasing temperature and vanished near T_c. Furthermore,
local impurities could also smear the feature as seen in the
spatially-resolved STS measurements. Figure 3(b) shows
the spectra measured along the trajectory of a 4-nm line
crossing a single impurity. It is obvious that when the
impurity states (behaving as a low-energy DOS peak)
appear and hence the superconducting order is suppressed,
the bosonic-excitation feature fades out. These data pro-
vide strong evidence that the bosonic mode is related to
superconductivity.

Although the observed bosonic mode is consistent with
the spin excitations in $Ba_{0.6}K_{0.4}Fe_2As_2$, one must also
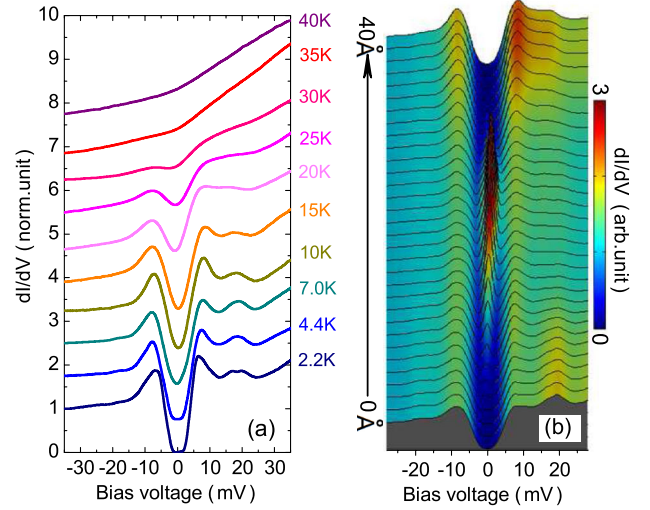consider phonon contributions. Experimentally, the

FIG. 3 (color online). (a) Temperature dependence of averaged
tunneling spectra. (b) Spatial dependence of tunneling spectra
taken along a line cutting through a local impurity, indicating the
close relationship between the strength of the hump-dip structure
and the superconducting order parameter.

phonon density of states of $BaFe_2As_2$ measured by neutron
scattering shows a clear peak near 12 meV that has been
identified as mostly arising from Ba vibrations [43,44].
Upon K doping to $Ba_{0.73}K_{0.27}Fe_2As_2$, the phonon modes
near $E = 10$–15 meV soften and broaden, but do not dis-
play any anomaly across the superconducting transition
temperature T_c [45]. The bosonic mode observed in our
STS study has a close relationship with superconductivity
and thus could not be the Ba-phonon modes that are not
related to superconductivity. Moreover, the phonon modes
related to the Fe-As layer have an energy scale of approxi-
mately 32 meV [43,44], which is much higher than the
energy of the bosonic mode observed here. In addition,
ARPES data indicate that only some bands show signature
of the mode around 13 meV, which is a strong argument
against a phononic origin (Ref. [46]).

Figures 4(a) and 4(b) show spatial distributions of the
superconducting gap and spin-excitation mode energy (Ω),
respectively (the figures are plotted in the same way as that
in Ref. [47]). The similar patterns of the Δ map and Ω map
indicate that Ω is locally anticorrelated with Δ [note that
the color bar is reversed in Fig. 4(b)]. This phenomenon is
universal for all the regions observed here. The strong local
anticorrelation suggests that the bosonic mode observed
here is an electronic excitation with an intrinsic origin
rather than a phonon mode or other extrinsic inelastic
excitation unrelated to superconductivity.

It should be emphasized that the anticorrelation is local
with a characteristic length of less than 2 nm and does not
indicate an anticorrelation between bulk superconductivity
(T_c or bulk-averaged superconducting gap) and bulk-
averaged spin-excitation energy. Such local anticorrelation
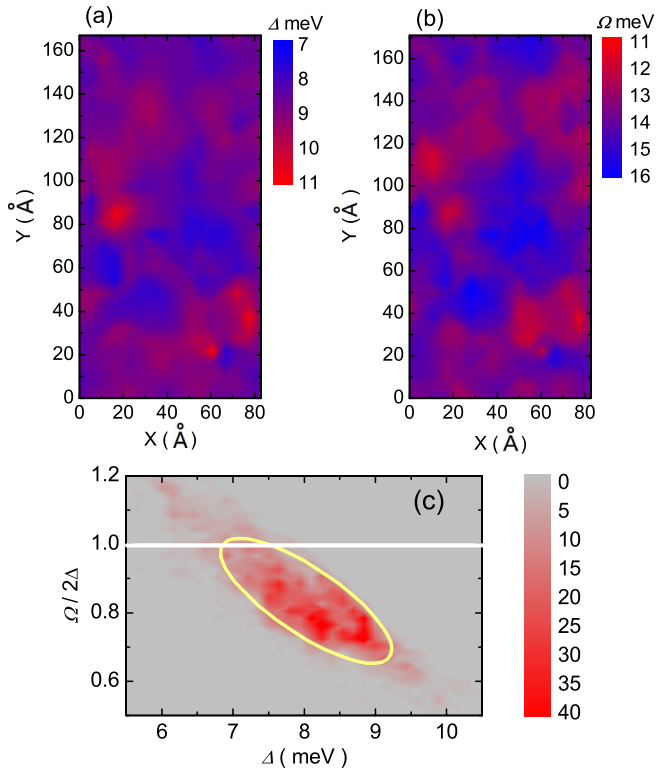is not accidental and has been observed in electron-doped

FIG. 4 (color online). (a) Image of the superconducting gap values, or gap map [$\Delta(r)$]. (b) Image of the mode energy $\Omega(r) = E_{dip}(r) - \Delta(r)$. Both (a) and (b) were obtained in the same region as mentioned in Figs. 1 and 2. (c) Histogram of the occurrences of Ω plotted as a local ratio $\Omega(r)/2\Delta(r)$ against $\Delta(r)$.

copper oxide superconductors [10,12]. In addition, in these electron-doped cuprates, direct correlation between bulk superconductivity and bulk-averaged spin-excitation energy was observed simultaneously [12]. This is consistent with the data from break junction tunneling obtained on hole-doped copper oxide superconductors $Bi_2Sr_2CaCu_2O_{8+\delta}$ (Bi2212) [14], in which a high-bias feature in the tunneling spectrum was also ascribed to the resonance spin excitation [14]. Furthermore, a quantitative Eliashberg analysis of the Bi2212 data was done to extract the electron-boson spectral function, $\alpha^2F(\omega)$, suggesting a narrow boson spectrum as paring glue [15,16], consistent with the results of optical conductivity [9]. This encourages us to relate the observed single dip in the spectrum of d^2I/dV^2 vs. V to a single, strong peak in $\alpha^2F(\omega)$. More interestingly, the ratio of $\Omega/2\Delta$ is always less than 1 for both hole-doped copper oxides and their electron-doped counterparts [10,14,48], consistent with a magnetic exciton in the spin-fermion type models [8,49]. This is very similar to our data with $\Omega/2\Delta$ below 1 for a statistically significant fraction as shown in Fig. 4(c). Moreover, in the framework of a four-band Eliashberg model, a combined description of the specific heat and far-infrared optical conductivity of optimally doped $Ba_{0.68}K_{0.32}Fe_2As_2$ clearly requires the

spectrum of the mediating boson to be centered around 13 meV (Refs. [50,51]) in full agreement with the present work. At present, a quantitative Eliashberg analysis of the tunneling data for iron-based superconductors is difficult to carry out due to the multiband nature of these materials. Nevertheless, the observation of a strong coupling between the spin resonance and electron tunneling spectra in both the iron- and copper-based superconductors, in spite of their dramatically different parent compounds (semimetals for iron-based superconductors and Mott insulators for copper oxide superconductors), suggests that electron-spin coupling is an important general feature of these materials.

In summary, we have discovered a bosonic excitation in the spatially-resolved tunneling spectra of the hole-doped iron-based superconductor $Ba_{0.6}K_{0.4}Fe_2As_2$. This mode occurs near 14 meV and has a close relationship with the superconducting order parameter. Because the mode energy is very close to the neutron spin resonance, we argue that the resonance must arise from quasiparticle excitations between the inner α-hole pocket and the electron pocket. This spin resonance mode is similar to that observed in copper oxide superconductors, supporting the idea that the spin fluctuation mechanism may be a generic characteristic of high-T_c superconductors.

*lshan@aphy.iphy.ac.cn
[1] G. M. Eliashberg, Sov. Phys. JETP **11**, 696 (1960).
[2] J. R. Schrieffer, D. J. Scalapino, and J. W. Wilkins, Phys. Rev. Lett. **10**, 336 (1963).
[3] W. L. McMillan and J. M. Rowell, Phys. Rev. Lett. **14**, 108 (1965).
[4] T. A. Maier, D. Poilblanc, and D. J. Scalapino, Phys. Rev. Lett. **100**, 237001 (2008).
[5] J. Bardeen, L. N. Cooper, and J. R. Schrieffer, Phys. Rev. **108**, 1175 (1957).
[6] P. Monthoux, D. Pines, and G. G. Lonzarich, Nature (London) **450**, 1177 (2007).
[7] T. Moriya and K. Ueda, Rep. Prog. Phys. **66**, 1299 (2003).
[8] M. Eschrig, Adv. Phys. **55**, 47 (2006).
[9] J. P. Carbotte, T. Timusk, and J. Hwang, Rep. Prog. Phys. **74**, 066501 (2011).
[10] F. C. Niestemski, S. Kunwar, S. Zhou, S. Li, H. Ding, Z. Wang, P. Dai, and V. Madhavan, Nature (London) **450**, 1058 (2007).

[11] S. D. Wilson, P. Dai, S. Li, S. Chi, H. J. Kang, and J. W. Lynn, Nature (London) **442**, 59 (2006).

[12] J. Zhao, F. C. Niestemski, S. Kunwar, S. Li, P. Steffens, A. Hiess, H. J. Kang, S. D. Wilson, Z. Wang, and P. Dai *et al.*, Nature Phys. **7**, 719 (2011).

[13] K. Jin, N. P. Butch, K. Kirshenbaum, J. Paglione, and R. L. Greene, Nature (London) **476**, 73 (2011).

[14] J. F. Zasadzinski, L. Ozyuzer, N. Miyakawa, K. E. Gray, D. G. Hinks, and C. Kendziora, Phys. Rev. Lett. **87**, 067005 (2001).

[15] J. F. Zasadzinski, L. Ozyuzer, L. Coffey, K. E. Gray, D. G. Hinks, and C. Kendziora, Phys. Rev. Lett. **96**, 017004 (2006).

[16] O. Ahmadi, L. Coffey, J. F. Zasadzinski, N. Miyakawa, and L. Ozyuzer, Phys. Rev. Lett. **106**, 167005 (2011).

[17] Y. Kamihara, T. Watanabe, M. Hirano, and H. Hosono, J. Am. Chem. Soc. **130**, 3296 (2008).

[18] X. H. Chen, T. Wu, G. Wu, R. H. Liu, H. Chen, and D. F. Fang, Nature (London) **453**, 761 (2008).

[19] H.-H. Wen, G. Mu, L. Fang, H. Yang, and X. Zhu, Europhys. Lett. **82**, 17 009 (2008).

[20] G. F. Chen, Z. Li, D. Wu, G. Li, W. Z. Hu, J. Dong, P. Zheng, J. L. Luo, and N. L. Wang, Phys. Rev. Lett. **100**, 247002 (2008).

[21] Z.-A. Ren, W. Lu, J. Yang, W. Yi, X.-L. Shen, Z.-C. Li, G.-C. Che, X.-L. Dong, L.-L. Sun, and F. Zhou *et al.*, Chin. Phys. Lett. **25**, 2215 (2008).

[22] M. Rotter, M. Tegel, and D. Johrendt, Phys. Rev. Lett. **101**, 107006 (2008).

[23] I. I. Mazin, Nature (London) **464**, 183 (2010).

[24] A. D. Christianson, E. A. Goremychkin, R. Osborn, S. Rosenkranz, M. D. Lumsden, C. D. Malliakas, I. S. Todorov, H. Claus, D. Y. Chung, and M. G. Kanatzidis *et al.*, Nature (London) **456**, 930 (2008).

[25] C. Zhang, M. Wang, H. Luo, M. Wang, M. Liu, J. Zhao, D. L. Abernathy, T. A. Maier, K. Marty, and M. D. Lumsden *et al.*, Sci. Rep. **1**, 115 (2011).

[26] Y. Fasano, I. Maggio-Aprile, N. D. Zhigadlo, S. Katrych, J. Karpinski, and O. Fischer, Phys. Rev. Lett. **105**, 167005 (2010).

[27] H. Luo, Z. Wang, H. Yang, P. Cheng, X. Zhu, and H.-H. Wen, Supercond. Sci. Technol. **21**, 125014 (2008).

[28] L. Shan, Y.-L. Wang, B. Shen, B. Zeng, Y. Huang, A. Li, D. Wang, H. Yang, C. Ren, and Q.-H. Wang *et al.*, Nature Phys. **7**, 325 (2011).

[29] L. Shan, Y.-L. Wang, J. Gong, B. Shen, Y. Huang, H. Yang, C. Ren, and H.-H. Wen, Phys. Rev. B **83**, 060510 (2011).

[30] J. E. Hoffman, Rep. Prog. Phys. **74**, 124513 (2011).

[31] T. Kato, Y. Mizuguchi, H. Nakamura, T. Machida, H. Sakata, and Y. Takano, Phys. Rev. B **80**, 180507 (2009).

[32] Y. Yin, M. Zech, T. L. Williams, X. F. Wang, G. Wu, X. H. Chen, and J. E. Hoffman, Phys. Rev. Lett. **102**, 097002 (2009).

[33] T. Hanaguri, S. Niitaka, K. Kuroki, and H. Takagi, Science **328**, 474 (2010).

[34] C.-L. Song, Y.-L. Wang, P. Cheng, Y.-P. Jiang, W. Li, T. Zhang, Z. Li, K. He, L. Wang, and J.-F. Jia *et al.*, Science **332**, 1410 (2011).

[35] M. L. Teague, G. K. Drayna, G. P. Lockhart, P. Cheng, B. Shen, H. H. Wen, and N. C. Yeh, Phys. Rev. Lett. **106**, 087004 (2011).

[36] See Supplemental Material at http://link.aps.org/supplemental/10.1103/PhysRevLett.108.227002 for details.

[37] W. McMillan and J. Rowell, *Superconductivity*, edited by R. D. Parks (Dekker, New York, 1969).

[38] E. Wolf, *Principles of Electron Tunneling Spectroscopy* (Oxford University Press, Oxford, 1985).

[39] Ø. Fischer, M. Kugler, I. Maggio-Aprile, C. Berthod, and C. Renner, Rev. Mod. Phys. **79**, 353 (2007).

[40] H. Ding, P. Richard, K. Nakayama, K. Sugawara, T. Arakane, Y. Sekiba, A. Takayama, S. Souma, T. Sato, and T. Takahashi *et al.*, Europhys. Lett. **83**, 47001 (2008).

[41] L. Zhao, H.-Y. Liu, W.-T. Zhang, J.-Q. Meng, X.-W. Jia, G.-D. Liu, X.-L. Dong, G.-F. Chen, J.-L. Luo, and N.-L. Wang *et al.*, Chin. Phys. Lett. **25**, 4402 (2008).

[42] J. Tersoff and D. R. Hamann, Phys. Rev. Lett. **50**, 1998 (1983).

[43] R. Mittal, Y. Su, S. Rols, T. Chatterji, S. L. Chaplot, H. Schober, M. Rotter, D. Johrendt, and T. Brueckel, Phys. Rev. B **78**, 104514 (2008).

[44] M. Zbiri, H. Schober, M. R. Johnson, S. Rols, R. Mittal, Y. Su, M. Rotter, and D. Johrendt, Phys. Rev. B **79**, 064511 (2009).

[45] C.-H. Lee, K. Kihou, K. Horigane, S. Tsutsui, T. Fukuda, H. Eisaki, A. Iyo, H. Yamaguchi, A. Q. R. Baron, and M. Braden *et al.*, J. Phys. Soc. Jpn. **79**, 014714 (2010).

[46] P. Richard, T. Sato, K. Nakayama, S. Souma, T. Takahashi, Y.-M. Xu, G. F. Chen, J. L. Luo, N. L. Wang, and H. Ding, Phys. Rev. Lett. **102**, 047003 (2009).

[47] J. Lee, K. Fujita, K. McElroy, J. A. Slezak, M. Wang, Y. Aiura, H. Bando, M. Ishikado, T. Masui, and J. X. Zhu *et al.*, Nature (London) **442**, 546 (2006).

[48] G. Yu, Y. Li, E. M. Motoyama, and M. Greven, Nature Phys. **5**, 873 (2009).

[49] A. Abanov and A. V. Chubukov, Phys. Rev. Lett. **83**, 1652 (1999).

[50] P. Popovich, A. V. Boris, O. V. Dolgov, A. A. Golubov, D. L. Sun, C. T. Lin, R. K. Kremer, and B. Keimer, Phys. Rev. Lett. **105**, 027003 (2010).

[51] A. Charnukha, O. V. Dolgov, A. A. Golubov, Y. Matiks, D. L. Sun, C. T. Lin, B. Keimer, and A. V. Boris, Phys. Rev. B **84**, 174511 (2011).